Path-reversed Auger electron and photoelectron diffraction

M. D. Pauli and D. K. Saldin
Department of Physics and Laboratory for Surface Studies, University of Wisconsin-Milwaukee, P.O. Box 413, Milwaukee, Wisconsin 53201
(Received 28 December 2000; published 25 July 2001)

We propose a method for the computer simulation of Auger electron and photoelectron diffraction patterns by evaluating the amplitude of propagation paths from the detector to the electron-emitting source, justified by Helmholtz's reciprocity principle. The method offers significant computational advantages over previous schemes, and suggests an easy extension to enable the calculation of a structure-perturbation tensor for rapid crystallographic parameter variation.

DOI: 10.1103/PhysRevB.64.075411 PACS number(s): 61.14.Qp, 61.14.Dc

I. INTRODUCTION

The techniques of Auger electron diffraction (AED) and photoelectron diffraction (PED) have received increased interest in the past decade or so due to a number of significant developments. One is the increasing availability of third-generation synchrotron radiation sources, which greatly facilitate the measurements of such patterns. Another is the development of holographic and other methods for reconstructing directly from the diffraction patterns, the local crystallography around the emitter atoms close to the surface of the sample.[1]

Methods of simulating such diffraction patterns take on a great importance for the verification of structural models, whether suggested by chemical intuition or one of the modern direct methods. In general, these simulation techniques require the calculation of the multiple scattering of the Auger electron or photoelectron from its point of emission to the detector.

One of the advantages of AED and PED over standard crystallographic techniques is not only their chemical selectivity, but also that the short inelastic-scattering length of the emitted electrons makes such diffraction patterns sensitive only to the short-range order of the atoms in the vicinity of emitters close to the surface. This enlarges the scope of such techniques beyond highly ordered surfaces.

Current methods for performing such calculations may be classified into two broad classes: those in which the scatterers are modeled by a local cluster of atoms around an emitter atom,[2,3] as is most convenient for systems that lack long-range order, and the so-called *slab method*,[4] which assumes two-dimensional (2D) periodicity parallel to the surface. The latter employs the computational machinery of low-energy electron diffraction (LEED),[5] enables the inclusion of a much larger number of atomic scatterers, and allows for a natural incorporation of refraction boundary conditions at the surface.[6] Further, in common with the concentric-shell cluster method[3] the multiple-scattering paths in the slab calculations are summed to infinite order, and are thus fully converged.

The purpose of the present paper is to point out the advantages of an elegant alternative formalism, based on the reciprocity principle, first enunciated for optics by Helmholtz. This principle states that the detected amplitude at point B, of a unit signal from a source at a point A, is equal to that detected at A due to a unit signal from a source at B. It has been pointed out by, e.g., Bilhorn *et al.*[7] that the same principle applies to electron propagation. The result is independent of the details of the potential between the two points. It holds even if the potential is taken to be complex to represent the effects of inelastic scattering.

II. CONVENTIONAL THEORY

In theories of electron scattering from surfaces, this idea has previously been exploited for valence-band photoemission,[8,9] high-resolution electron energy loss spectroscopy,[10,11] diffuse LEED,[12] and tensor LEED.[13] Yet, surprisingly, to date it has not been employed for the calculation of core-level photoelectron diffraction. In this paper we demonstrate that there are several important advantages to the computation of the path-reversed process of the back propagation of a photoelectron from the position of a distant detector to that of the emitting atom compared to the physical process of propagation from the emitter to the detector.

We begin by considering the case of atomic core-level PED. The wave function of a photoelectron initially emitted by an atom s after its excitation from an atomic core state $\phi_{s,c}(\mathbf{r}')$ by (an electromagnetic) perturbation Δ may be written

$$\psi(\mathbf{r}'';E)=\int G_a^+(\mathbf{r}'',\mathbf{r}';E)\Delta(\mathbf{r}')\phi_{s,c}(\mathbf{r}')d\mathbf{r}', \qquad (1)$$

where $\mathbf{r}'$ and $\mathbf{r}''$ are position vectors (referred to an origin at the atom center for convenience) and $G_a^+(\mathbf{r}'',\mathbf{r}';E)$ is the retarded atomic Green function of the excited photoelectron of energy E. On a muffin-tin model of the crystal, where the interstitial potential inside the solid is represented by a real part V_{0r} and an imaginary one V_{0i}, the atomic Green function may be written (in Hartree atomic units):

$$G_a^+(\mathbf{r}'',\mathbf{r}';E)=-ik^{\mathrm{in}}\sum_{lm} R_l^+(r_>;E)Y_{lm}(\hat{\mathbf{r}}'') \times R_l(r_<;E)Y_{lm}^*(\hat{\mathbf{r}}'), \qquad (2)$$

where $k^{\mathrm{in}}=\sqrt{2(E-V_{0r}-iV_{0i})}$ is the electron wave number in the intersitial regions, R and R^+ are regular and irregular solutions of the radial Schrödinger equation for the atomic

potential, Y represents a spherical harmonic, and l and m are the azimuthal and magnetic quantum numbers, respectively. Substituting Eq. (2) into Eq. (1) and noting that R_l^+ matches onto $h_l^{(1)}(k^{\rm in}r'')\exp(i\delta_l)$ at the muffin-tin radius (where $h^{(1)}$ is a Hankel function of the first kind, and δ and atomic phase shift) we note that the wave function (1) may be written

$$\psi(\mathbf{r}'';E) = -ik^{\rm in}\sum_{lm} M_{s,lm,c}h_l^{(1)}(k^{\rm in}r'')Y_{lm}(\hat{\mathbf{r}}'')\exp(i\delta_l), \tag{3}$$

beyond the range of the atomic potential, where

$$M_{s,lm,c}(E) = \int R_l(\mathbf{r}';E)Y_{lm}^*(\hat{\mathbf{r}}')\Delta(\mathbf{r}')\phi_{s,c}(\mathbf{r}')d\mathbf{r}' \tag{4}$$

is the matrix element for the atomic transition, and $\phi_{s,c}$ the wave function of a core electron of atom s.

Traditional methods of calculating photoelectron diffraction further propagate this wave through the crystal to just inside its surface where it is projected into a state

$$\langle \mathbf{r}|\mathbf{k}_\parallel\rangle = \frac{1}{L}\exp(i\mathbf{k}_\parallel\cdot\mathbf{r})\,\delta(z-Z) \tag{5}$$

characterized by its wave vector component parallel to the surface, $\mathbf{k}_\parallel$, z is the component of $\mathbf{r}$ perpendicular to the surface of the material, Z defines a plane of observation, which may be taken as that of the surface, and L is a linear dimension of the experimental system. Since $\mathbf{k}_\parallel$ is conserved on the passage of the photoelectron through the surface into an external vacuum, the differential flux (w) per unit solid angle Ω of an electron with the same parallel component of wave vector registered at an external detector, may be written[6]

$$\frac{dw}{d\Omega}(\mathbf{k}_\parallel) = \frac{k^{\rm out}(k_z^{\rm out})^2}{(2\pi)^2}L^2\sum_s |B_s(\mathbf{k}_\parallel,E)|^2, \tag{6}$$

where

$$B_s(\mathbf{k}_\parallel,E) = \langle \mathbf{k}_\parallel|G^+(E)\Delta|\phi_{s,c}\rangle. \tag{7}$$

$G^+(E)$ is the complete propagator of the photoelectron from the excited atom to the detector, $k^{\rm out}=\sqrt{2E}$ is the wave number of the electron outside the sample, and $k_z^{\rm out}$ $[=\sqrt{(k_z^{\rm out})^2-\mathbf{k}_\parallel^2}]$ its component perpendicular to the surface. Note that the term L^2 in Eq. (6) is cancelled by the factors of $1/L$ from the state (5) in the matrix element B_s, and hence the differential flux (6) is independent of L.

III. PATH-REVERSED FORMALISM

In developing a path-reversed formulation, note first that one may expand $B_s(\mathbf{k}_\parallel,E)$ as

$$\int\int d\mathbf{r}'\,d\mathbf{r}\langle \mathbf{k}_\parallel|\mathbf{r}\rangle\langle\mathbf{r}|G^+(E)|\mathbf{r}'\rangle\Delta(\mathbf{r}')\langle\mathbf{r}'|\phi_{s,c}\rangle. \tag{8}$$

Now reversing the position indices of the propagator $G^{(+)}(E)$ (as justified by the reciprocity principle) and rearranging terms, we may rewrite this as

$$\int d\mathbf{r}'\left[\int d\mathbf{r}\langle\mathbf{r}'|G^{(+)}(E)|\mathbf{r}\rangle\langle\mathbf{r}|-\mathbf{k}_\parallel\rangle\right]\Delta(\mathbf{r}')\langle\mathbf{r}'|\phi_{s,c}\rangle. \tag{9}$$

The term within square brackets above may be thought of as the wave function at the site of the photoemitting atoms s due to the backpropagation through the crystal of a path-reversed plane wave from the source

$$\langle\mathbf{r}|-\mathbf{k}_\parallel\rangle = \frac{1}{L}\exp(-\mathbf{k}_\parallel\cdot\mathbf{r})\,\delta(z-Z) \tag{10}$$

at the surface of the sample. Before an encounter with any of the scattering atoms, this wave may be written

$$\langle\mathbf{r}|G^+(E)|-\mathbf{k}_\parallel\rangle = \frac{i}{2k_z^{\rm in}L}\exp(-i\mathbf{k}\cdot\mathbf{r}), \tag{11}$$

where $k_z^{\rm in}=\sqrt{(k^{\rm in})^2-\mathbf{k}_\parallel^2}$ is the component of $k^{\rm in}$ perpendicular to the surface. This may be regarded as a plane wave of amplitude $(i/2k_zL)$ incident on the sample. Its subsequent scattering and propagation is exactly like a LEED electron of that incident amplitude.[14] According to LEED theory, after backpropagation through the crystal, the final wave function incident on the original *photoemitter s* may be written

$$\begin{aligned}\langle\mathbf{r}''|G^+(E)|-\mathbf{k}_\parallel\rangle &= \frac{i}{2k_z^{\rm in}L}\sum_{lm} A_{s,lm}(-\mathbf{k}_\parallel)j_l(k^{\rm in}r'')Y_{lm}(\hat{\mathbf{r}}'')\\ &= \frac{i}{2k_z^{\rm in}L}\sum_{lm}(-)^m A_{s,l-m}(-\mathbf{k}_\parallel)\\ &\quad\times j_l(k^{\rm in}r'')Y_{lm}^*(\hat{\mathbf{r}}'').\end{aligned} \tag{12}$$

The amplitudes $A_{s,lm}(-\mathbf{k}_\parallel)$ are, for example, specifically calculated by the TLEED1 program of Rous and Pendry[15] at each inequivalent substrate atom s. The subsequent elastic scattering of the wave function (12) by the photoemitting atom adds an extra term $t_l h_l^{(1)}(\kappa r'')$ to the spherical Bessel function $j_l(\kappa r'')$ (where t_l is an element of the scattering t matrix of the atom). The resulting radial wave function matches onto $\exp(i\delta_l)R_l(r';E)$, where R_l is the same regular solution to the radial Schrödinger equation inside the muffin-tin radius as in Eq. (4). Consequently, from Eq. (9) we see that

$$\begin{aligned}B_s(\mathbf{k}_\parallel,E) &= \int d\mathbf{r}'\langle\mathbf{r}'|G^{(+)}(E)|-\mathbf{k}_\parallel\rangle\Delta(\mathbf{r}')\langle\mathbf{r}'|\phi_{s,c}\rangle\\ &= \frac{i}{2k_z^{\rm in}L}\sum_{lm}(-)^m A_{s,l-m}(-\mathbf{k}_\parallel)\exp(i\delta_l)\\ &\quad\times\int d\mathbf{r}'\,R_l(r',E)Y_{lm}^*(\hat{\mathbf{r}}')\Delta(\mathbf{r}')\phi_{s,c}(\mathbf{r}')\\ &= \frac{i}{2k_z^{\rm in}L}\sum_{lm}(-)^m\exp(i\delta_l)A_{s,l-m}(-\mathbf{k}_\parallel)M_{lm,c}(E)\end{aligned} \tag{13}$$

and the angle-resolved differential flux at a PED detector follows by substituting Eq. (13) into Eq. (6).

Almost exactly the same arguments hold for AED, except of course that the photoemission matrix element $M_{s,lm,c}(E)$ is replaced by that $Q_{s,lm,c}(E)$ for Auger emission, where c now stands for the set of three intermediate energy levels of an Auger process, and the energy E of the emitted electron is now determined by just those energy levels, and not that of the exciting radiation. In addition, in AED, the different angular momentum components of the emitted electrons are assumed to be mutually incoherent.[16] Thus, the angle-resolved differential flux in AED may be written

$$\frac{dw}{d\Omega}(\mathbf{k}_{\|}) = \frac{k^{\text{out}}}{4(2\pi)^2}\left(\frac{k_z^{\text{out}}}{k_z^{\text{in}}}\right)^2 \sum_{s,lm} |A_{s,l-m} Q_{s,lm,c}(E)|^2. \tag{14}$$

IV. COMPUTER SIMULATIONS AND COMPARISON WITH EXPERIMENT

We will describe practical calculations for PED in a future paper. Here we present the results of simulating some well-known AED patterns, which became something of a *cause célèbre* in the early 1990's during a brief controversy about their interpretation. Frank *et al.*[17,18] had proposed a classical blocking and shadowing model to interpret these patterns, but subsequent work[19] showed that a full quantum-mechanical multiple-scattering calculation reproduced the experimental patterns much better than the classical scattering models.[17,18] Perhaps of greater importance was the fact that this focused attention on the significantly different character of low-energy AED (and PED) patterns (<approximately 500 eV) in comparison with corresponding high-energy ones (>approximately 500 eV). As an example of the former, we consider the 64 eV $M_{2,3}VV$ AED pattern from a Cu(001) surface, and as for the latter the 914 eV $L_{2,3}VV$ one from the same surface.

Figures 1 and 2 illustrate simulations by our path-reversed formalism of the 64 and 914-eV AED patterns, respectively. In each case, the left-hand column shows the experimental pattern measured by Frank *et al.*,[18] while the other columns show the simulated patterns due to Auger electrons emitted into the *s*, *p*, *d*, *f*, and *g* angular momentum channels ($l=0$, 1, 2, 3, and 4, respectively). That is, these patterns were simulated by Eq. (14) with a single value of l in the summation, and where the values of the matrix elements $Q_{lm,c}$ are assumed to be equal for different m's, corresponding to a given l.

The simulations of the low-energy (64 eV) AED pattern (Fig. 1) of different emitted angular momentum channels are very different, and a mere visual inspection clearly indicates that only the *f*-wave pattern has any significant agreement with experiment.

In contrast, the high-energy (914 eV) Auger patterns of Fig. 2 are all dominated by strong *forward-scattering*[20] features close to the projections of atomic rows due to the strongly forward-peaked atomic scattering factors at such energies. Although the variation of the patterns with l are much smaller, a careful study of the simulated patterns indicates that the one due to the *f*-wave emitter agrees best with experiment.

Both sets of results are consistent with the selection rules[19] for these particular Auger transitions, which suggest that the matrix elements $Q_{lm,c}$ with $l=3$ dominate over all others. Also, a comparison of the computer simulated patterns of Figs. 1 and 2 with those of Chen, Harp, and Saldin[19] simulated by the concentric shell algorithm, shows remarkable agreement despite the radical differences between the algorithms.

V. DISCUSSION AND CONCLUSIONS

We draw attention to a significant advantage of the path-reversed formalism over any of the previous methods. In cases, such as those illustrated here, where AED or PED patterns are formed by a superposition of those due to a large number of inequivalent emitters, the previous ''time-forward'' methods require a separate multiple-scattering calculation for each emitter. In contrast, in our path-reversed calculation, a single LEED multiple-scattering calculation gives the $A_{s,l-m}$ coefficients for all inequivalent emitters s. Hence the task of generating the entire AED or PED pattern

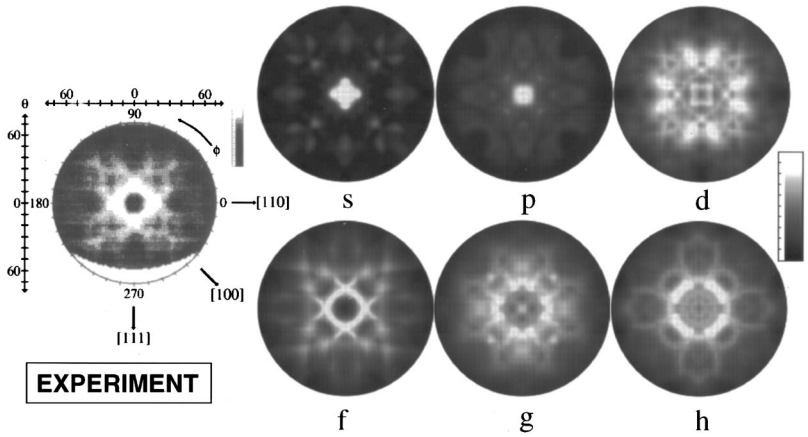

FIG. 1. Simulations by our path-reversed method of 64 eV AED patterns from a Cu(001) surface for different angular momentum channels (*s*, *p*, *d*, *f*, *g*, and *h*) of the emitted Auger electron. Also shown is the corresponding experimental $M_{2,3}VV$ AED pattern reproduced from the paper of Frank *et al.* (Ref. [18]).

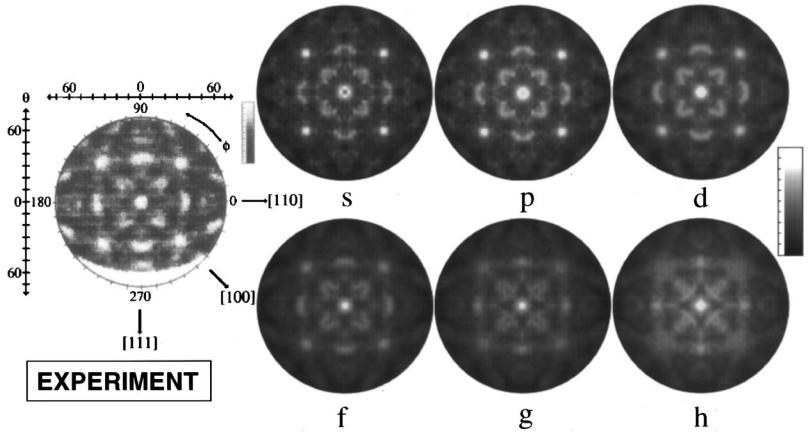

FIG. 2. The same as Fig. 1, except that the diffraction patterns are those of 914 eV $L_{2,3}VV$ Auger electrons, also as measured by Frank *et al.* (Ref. 18).

is a simple matter of summing terms of the form (13) or (14) for each emitter, where all quantities are computed in a single pass of the algorithm. This could potentially speed up such calculations by an order of magnitude or more.

One of the drawbacks of using AED or PED to accurately determine crystallographic parameters is the lack, up to the present, of a widely available scheme, such as the tensor LEED method,[15] for rapidly simulating the diffraction patterns of a large number of closely related structures. Crucial elements in the construction of this *structure perturbation tensor* are the very amplitudes $A_{s,lm}$ that form the centerpiece of our present method. This provides a very convenient framework for the incorporation of future tensor-LEED type enhancements to allow AED and PED to reach their full potential as (chemically selective) techniques for surface crystallography.

ACKNOWLEDGMENTS

The authors acknowledge stimulating discussions with A. Wander and H.-C. Poon, and financial support from the U.S. Department of Energy (Grant No. DE-FG02-84ER45076) and the U.S. National Science Foundation (Grant Nos. DMR-9815092 and 9972958-001).

[1] For a recent review, see, e.g., C. S. Fadley, M. A. Van Hove, Z. Hussain, A. P. Kaduwela, R. E. Crouch, Y. J. Kim, P. M. Len, J. Palomares, S. Ryce, S. Ruebush, E. D. Tober, Z. Wang, R. X. Ynzunza, H. Daimon, H. Galloway, M. B. Salmeron, and W. Schattke, Surf. Rev. Lett. **4**, 421 (1997).

[2] A. P. Kaduwela, G. S. Herman, D. J. Friedman, and C. S. Fadley, Phys. Scr. **41**, 948 (1990) as based on a method described in J. J. Rehr and R. C. Albers, Phys. Rev. B **41**, 81 139 (1990).

[3] D. K. Saldin, G. R. Harp, and X. Chen, Phys. Rev. B **48**, 8234 (1993).

[4] C. H. Li, A. R. Lubinsky, and S. Y. Tong, Phys. Rev. B **17**, 3128 (1978).

[5] M. A. Van Hove and S. Y. Tong, *Surface Crystallography by LEED* (Springer-Verlag, Heidelberg, 1979).

[6] H. Wu, C. Y. Ng, T. P. Chu, and S. Y. Tong, Phys. Rev. B **57**, 15 467 (1998).

[7] D. A. Bilhorn, L. L. Folder, R. M. Thaler, and W. Tobocman, J. Math. Phys. **5**, 435 (1964).

[8] J. B. Pendry, Surf. Sci. **57**, 679 (1976).

[9] J. F. L. Hopkinson, J. B. Pendry, and D. J. Titterington, Comput. Phys. Commun. **19**, 69 (1980).

[10] S. Y. Tong, C. H. Li, and D. L. Mills, Phys. Rev. Lett. **44**, 407 (1980).

[11] G. C. Aers, J. B. Pendry, T. B. Grimley, and K. L. Sebastian, J. Phys. C **14**, 3995 (1981).

[12] D. K. Saldin and J. B. Pendry, Comput. Phys. Commun. **42**, 399 (1986).

[13] P. J. Rous and J. B. Pendry, Comput. Phys. Commun. **54**, 137 (1989).

[14] The resulting state has been termed a ''time-reversed LEED state'' in the literature. This is a slight misnomer in the presence of absorption, since the true time reverse of an attenuated wave is one whose amplitude *increases* exponentially along the reverse path. In the quoted ''time-reversed LEED states,'' the path-reversed amplitudes are attenuated, just as the true physical ones traversing the reverse direction. The reciprocity theorem holds even in the presence of such reciprocal attenuantion processes.

[15] (a) P. J. Rous and J. B. Pendry, Comput. Phys. Commun. **54**, 137 (1989); (b) **54**, 157 (1989).

[16] D. K. Saldin, G. R. Harp, and B. P. Tonner, Phys. Rev. B **45**, 9629 (1992).

[17] D. G. Frank, N. Batina, T. Golden, F. Lu, and A. T. Hubbard, Science **247**, 182 (1990).

[18] D. G. Frank, T. Golden, O. M. R. Chyan, and A. T. Hubbard, J. Vac. Sci. Technol. A **9**, 1254 (1990).

[19] For example, X. Chen, G. R. Harp, and D. K. Saldin, J. Vac. Sci. Technol. A **12**, 428 (1994).

[20] H. C. Poon and S. Y. Tong, Phys. Rev. B **30**, 6211 (1984).